

# Core Neutronic Characterization of Advanced Pressurized Water Reactor

Hend Saad<sup>1,\*</sup>, Moustafa Aziz<sup>1</sup>, Riham Refeat<sup>1</sup>, Hesham Mansour<sup>2</sup>

<sup>1</sup>Nuclear Safety Engineering Department, Nuclear and Radiological Regulatory Authority, 3 Ahmed El Zomor St., Nasr City, Cairo, Egypt  
<sup>2</sup>Physics Department, Faculty of Science, Cairo University, Giza, Egypt

**Abstract** Based on design improvements and operational experience to conventional PWRs, the advanced PWR (APWR) has been attained for use as a standard large-scale plant. Developments have been made to improve the economical efficiency, safety, and reliability by various design improvements, such as reactor core enlargement and an increase in the burnup of fuel. In this paper, MCNP6 computer code is used to model the reactor core of Advanced Pressurized Water Reactor (APWR). The reactor core, consisting of 257 improved 17 x 17 fuel assemblies, has a thermal output of approximately 4451 MWt. The effective multiplication factor of the core and radial power mapping distributions are calculated and compared with the reference. The depletion of fissile materials U-235, U-238, Pu-238, Pu-239, Pu-241, and Pu-242 is determined at different Burnup steps. Kinetic parameters such as delayed neutron fractions and prompt neutron life time are determined and compared also with the reference. Good agreement is observed between the present model and the reference in all cases.

**Keywords** Advanced Pressurized Water Reactor (US-APWR), Burnable poisons, Gadolinium (Gd), Burnup, and radial power distribution

## 1. Introduction

The Advanced Pressurized Water Reactor APWR has been developed, as a joint international cooperative development project between the Japanese PWR electric power companies, Mitsubishi Heavy Industries and Westinghouse. APWR is a generation III nuclear reactor design developed based on advanced pressurized water reactor technology [1]. Generation III nuclear reactors are essentially generation II reactors with evolutionary design improvements in several areas, namely, fuel technology, thermal efficiency, modularized construction, safety systems, and standardized design for each type. These improvements are undergone to expedite licensing, reduce the capital cost and construction time. Generation III improvements in reactor technology have aimed at a longer operational life, typically 60 years of operation. A simpler and more rugged design makes them easier to operate and less vulnerable to operational upsets. Further, it reduced possibility of core melt accidents. Higher burn-up of fuel increases its efficiency, and reduce the amount of waste produced. Greater use of burnable absorbers ('poisons') to extend fuel life [2]. The basic design concepts of the US-APWR are similar to those of Japanese APWR whose

design has completed. Namely; the US-APWR has been developed as a large-scale version for the advanced pressurized water reactor, aiming at higher electrical outputs and improved economics [1]. US-APWR has a 4451 MWt, about 1600 MWe net, due to longer (4.3m instead of 3.7m in earlier designed PWR) fuel assemblies, higher core burnup and higher thermal efficiency (37%). It has 24-month fuel cycle. The most important requirement of a nuclear power plant is the safety, so, the US-APWR incorporates numerous technical improvements to further enhance its safety features [3-6].

## 2. Reactor Core Description

The US-APWR core consists of 257 fuel assemblies surrounded by a stainless-steel radial neutron reflector designed to improve neutron utilization, which reduces the fuel cycle cost and significantly reduces reactor vessel irradiation compared to previous PWRs with baffle/barrel designs [1]. The 17 x 17 fuel assembly consists of 264 fuel rods, 24 guide thimble tubes, and 1 instrumentation thimble tube. The instrumentation thimble is positioned in the center of the fuel assembly to provide a location for an in-core neutron detector if the fuel assembly is located in an instrumented core position as shown in figure (1). The radial reflector, consisting of stainless steel blocks, not only reduces fuel cycle costs but also reduces the irradiation of the reactor vessel and core internals. Through installation of the radial reflector, neutron irradiation of the reactor vessel can

\* Corresponding author:

hendmohammed\_science@yahoo.com (Hend Saad)

Received: Nov. 10, 2020; Accepted: Dec. 6, 2020; Published: Mar. 20, 2021

Published online at <http://journal.sapub.org/jnpp>

be reduced to 1/3 that of present reactors. The US-APWR, with a low power density core, not only reduces the number of fuel assembly replacements, which improves fuel economic efficiency, but also enables the long-cycle operation of about 24 months, leading to better availability and reduction of generation costs.

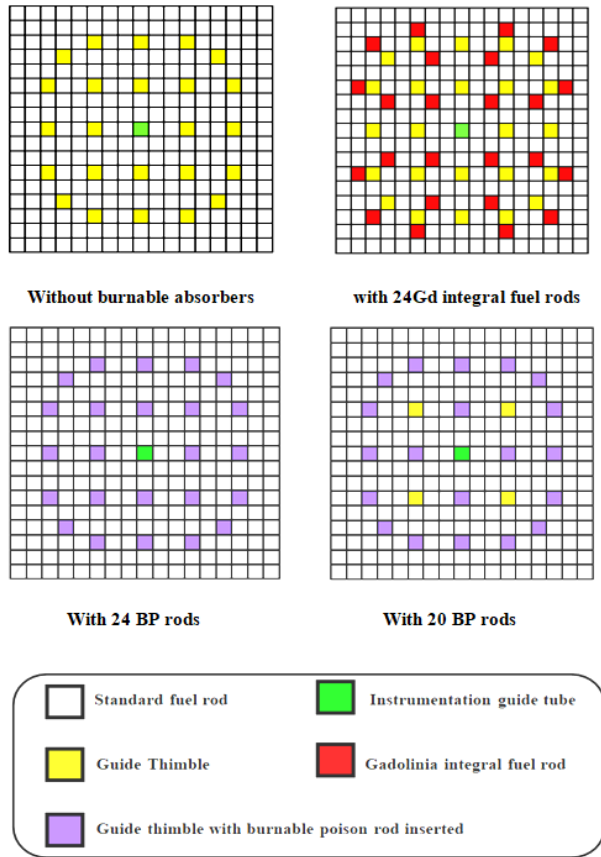


**Figure 1.** Arrangement of Fuel and Burnable Poison Rods within fuel assembly (initial core)

The fuel rod consists of ZIRLO<sup>TM</sup><sup>1</sup> fuel cladding loaded with sintered uranium dioxide pellets and/or sintered Gadolinia-uranium dioxide pellets, a coil spring in the upper plenum, a lower plenum spacer, and end plugs welded at the top and bottom ends to seal the rod. To reduce pellet/cladding interaction and prevent collapse during normal operation, the fuel rods are pressurized with helium through a pressurization hole provided in the top end plug which is then closed off by welding to yield a sealed structure; with upper and lower plenums has enough free volume to accommodate the fission gas release.

Some fuel rods are mixed axially with Gd<sub>2</sub>O<sub>3</sub> (Gadolinium oxide) to form Gadolinia rods. Figure 2 illustrates the axial composition of fuel rods and three models of Gadolinia rods are used:

Model (A): The active fuel zone is filled with pure UO<sub>2</sub> pellets.

Model (B): The upper part of the fuel (15.24 cm or 6 inches) is UO<sub>2</sub> and lower part (UO<sub>2</sub> + Gd<sub>2</sub>O<sub>3</sub>) pellets.

Model (C): contain three parts the upper and lower part is UO<sub>2</sub> (which are different in thickness) while (UO<sub>2</sub> + Gd<sub>2</sub>O<sub>3</sub>) in between.

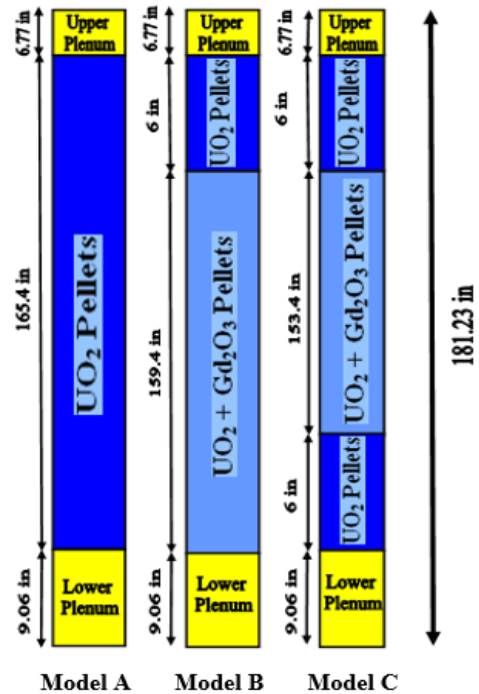


**Figure 2.** Schematic View of axial composition of Fuel Rod (Dimensions in inches according to the reference)

Figure 3 shows a typical initial core loading pattern. The core consists of 257 assemblies distributed in 9 different batches as indicated in first column of Figure 3. Each batch consists of a number of similar assemblies. Each assembly batch is characterized by different fuel enrichment, axial rods composition, number of burnable poison and rod Gadolinium content. Further details can be found at reference [1]. The core is summarized in the nine batches as:

- **R1UA:** The assembly contains 264 fuel rods of model (A) with initial enrichment 2.05% without Burnable poisons or Gadolinia.
- **R2UA:** The assembly contains 264 fuel rods of model (A) with initial enrichment 3.55% without Burnable poisons or Gadolinia.
- **R2UC:** The assembly contains 264 fuel rods of model (A) with initial enrichment 3.55% and 20 Burnable poisons without Gadolinia.
- **R2UD:** The assembly contains 264 fuel rods of model (A) with initial enrichment 3.55% and 24 Burnable poisons without Gadolinia.
- **R2GB:** The assembly contains 240 fuel rods with initial enrichment 3.55% and 24 Gadolinia fuel rods of model (B) and without Burnable poisons.
- **R2GC:** The assembly contains 240 fuel rods with initial enrichment 3.55% and 24 Gadolinia fuel rods of model (B) and without Burnable poisons.

<sup>1</sup> ZIRLO<sup>TM</sup> is a registered trademark of the Westinghouse Electric Corporation.



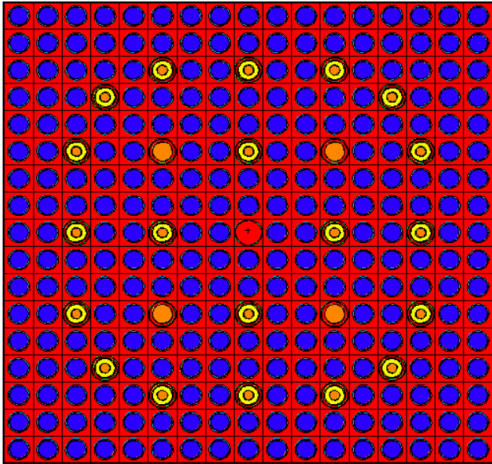


Figure 6. An MCNP6 cross sectional view for model (A), with 20 burnable absorbers

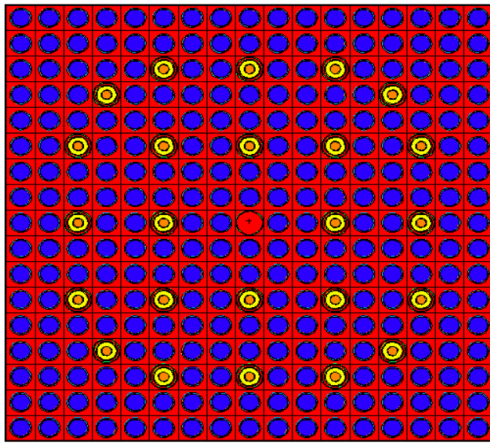


Figure 7. An MCNP6 cross sectional view for model (A), with 24 burnable absorbers

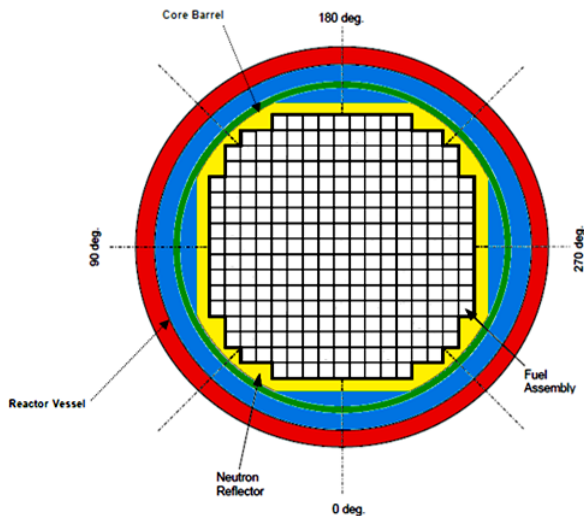


Figure 8. MCNP6 cross sectional view of radial Initial Core Fuel Loading Patterns

### 4. Results and Discussion

The effective multiplication factor of the reactor is

calculated for the initial core [1]. The initial conditions used: temperature of cold shutdown, without xenon (NoXe), all control rods are out (ARO), no soluble boron (zero ppm), for beginning of cycle (BOC). Using MCNP6 code and library ENDF/B-VII.1 [9] the maximum core  $K_{eff}$  of the present work is shown in table 1. It is noticed that the difference between the present model and the reference [1] is 47pcm with estimated relative error equal to 0.00043. The result shows a good agreement. This indicated that the current version of MCNP6 and the nuclear data library used (ENDF/B-VII.1), can accurately simulate the US-APWR.

Table 1. The Maximum core  $k_{eff}$  for initial core

US-APWR Core	Present Model	Reference [1]
<b>Multiplication Factor</b>	1.22347	1.223

In the next sections, the radial power distribution is determined and analyzed. Then, the Burnup calculations are determined for the initial core.

#### 4.1. Radial Power Distribution

Power distribution for typical initial core (one-eighth-core) normalized radial power distribution at hot full power, without xenon (NoXe) conditions for beginning of cycle (BOC) is shown in Figure 9. The upper value is the assembly type; the second is the power value for the present model, third for Reference, followed by difference between the present model and reference. The average difference between the present model and the reference is 0.0583 with minimum difference 0.01 and maximum difference 0.11 for two assemblies only.

Region	Present model	Reference	Diff.			
R1UA	0.70	0.78	0.10			
R2GC	R1UA	0.76	0.77			
		0.86	0.82			
		0.11	0.06			
R1UA	R3GB	R1UA				
		0.79	0.96			
		0.83	0.99			
		0.05	0.03			
R3GB	R1UA	R3GB	R1UA			
		0.99	0.90			
		0.98	0.88			
		0.01	0.02			
R2GB	R3GC	R1UA	R2GC	R1UA		
		0.92	1.03	0.87		
		0.88	1.05	0.92		
		0.05	0.02	0.05		
R3GC	R1UA	R3GC	R1UA	R2UD	R1UA	
		1.16	0.90	1.12	1.14	
		1.07	0.94	1.10	0.95	
		0.08	0.04	0.02	0.03	
R1UA	R3GB	R1UA	R2GB	R3GC	R2UD	R1UA
		1.04	1.10	0.96	0.97	1.13
		0.96	1.07	0.92	0.96	1.14
		0.08	0.03	0.04	0.01	0.01
R1UA	R3GB	R2GB	R3GB	R2UC	R2UA	R2UA
		1.09	1.13	1.06	0.97	1.06
		0.98	1.06	0.97	1.06	1.08
		0.11	0.07	0.09	0.08	0.02
R1UA	R3UA	R2UA	R2UA	R3UA		
		0.83	1.20	0.94	0.94	0.91
		0.75	1.11	1.06	1.05	0.93
		0.11	0.08	0.11	0.10	0.02

(HFP, NoXe, ARO)

Figure 9. Normalized Radial Power at 0 (GWD/MTU)

### 4.2. Burnup Calculation

The core is burned up to 40 (GWd/MTU). The values of the  $k_{eff}$  obtained for whole core are presented in Figure 10.

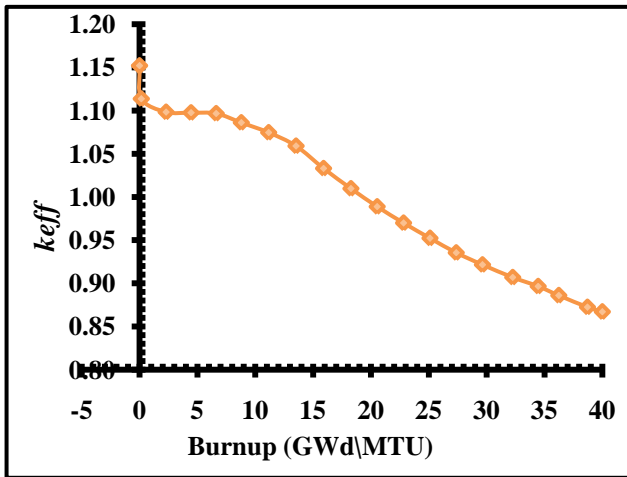


Figure 10. Variation of  $k_{eff}$  of the core with burnup

The full core is burned up to [40 GWd/MTU]. The values of the  $k_{eff}$  obtained for whole core are presented in Figure 10.  $K_{eff}$  behavior with burnup can be divided into 3 modes: at the beginning decreases largely due to  $^{135}X$  buildup, below 18 (GWd/MTU)  $K_{eff}$  decreases slowly because of burnable poisons and after 18 (GWd/MTU), the rate increases after burnup of burnable poisons.

Figure 11 illustrates  $K_{eff}$  versus operation times (days) corresponding to figure 10 the results indicate that the reactor could achieve full cycle length of 24 months.

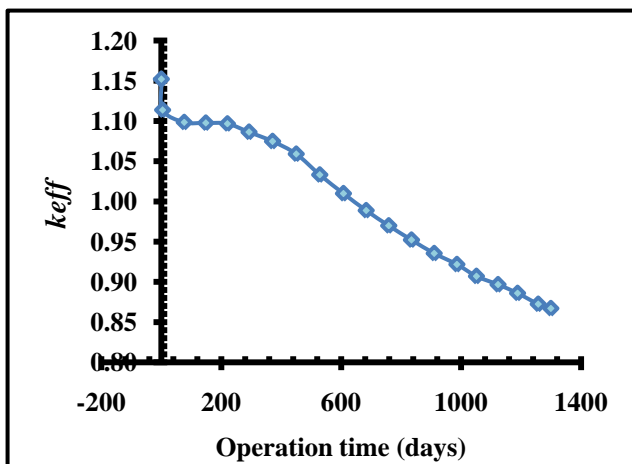


Figure 11.  $k_{eff}$  change with time of full core

Figure 12: shows the concentration (atom density) of  $^{235}U$  nuclides (atoms/barn.cm) versus burnup (GWd/MTU) averaged over the full core. The initial concentration of  $^{235}U$  is  $6.318E-04$  (atoms/barn.cm) and at fuel burn up of 40 GWd/MTU is  $1.979E-04$  (atoms/barn.cm), which indicate that 68.6% of  $^{235}U$  are consumed during this period.

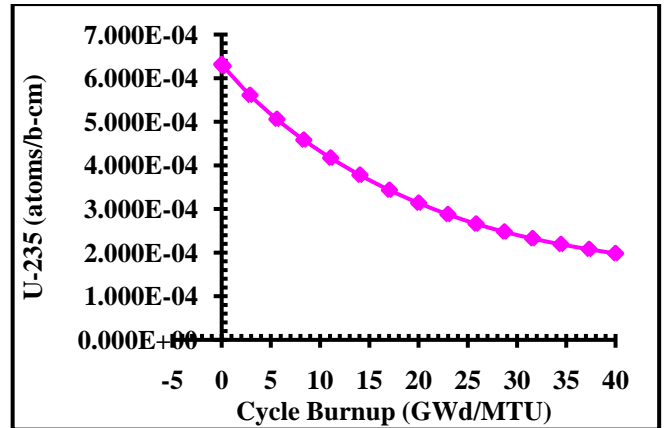


Figure 12.  $^{235}U$  concentration (atoms/barn-cm) with burnup (GWd/MTU) averaged over full core

Figure 13: shows the concentration (atom density) of  $^{238}U$  nuclides (atoms/barn.cm) versus burnup (GWd/MTU). The initial concentration of  $^{238}U$  is  $2.212E-02$  (atoms/barn.cm) and at fuel burn up of 40 (GWd/MTU) is  $2.132E-02$  (atoms/barn.cm), which indicates that 3.6% are consumed.

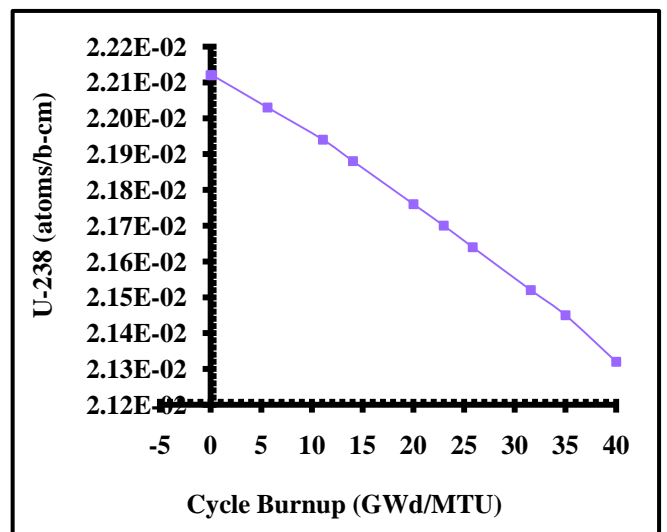


Figure 13.  $^{238}U$  concentration (atoms/barn-cm) with burnup (GWd/MTU) averaged over full core

Figure 14: shows the concentration of plutonium isotopes (atoms/ barn.cm) versus cycle burnup (GWd/MTU). The plutonium isotopes built up from zero for fresh  $UO_2$  fuel and increased with time as the fuel burnt and seemed to reach stability. The  $^{239}Pu$  also approached equilibrium because at higher burnup, the rate of  $^{239}Pu$  production equaled the rate of neutron absorption and fission. At 0.15 (GWd/MTU), the concentration of  $^{238}Pu$  is  $1.029E-12$ ,  $^{239}Pu$  is  $8.414E-07$ ,  $^{240}Pu$  is  $1.032E-08$ ,  $^{241}Pu$  is  $3.771E-10$ , and  $^{242}Pu$  is  $2.850E-12$  (atoms/barn.cm). Although at 40 (GWd/MTU), the concentration of  $^{238}Pu$  is  $5.507E-06$ ,  $^{239}Pu$  is  $9.231E-05$ ,  $^{240}Pu$  is  $4.954E-05$ ,  $^{241}Pu$  is  $2.432E-05$  and of  $^{242}Pu$  is  $2.271E-05$  (atoms/barn.cm).

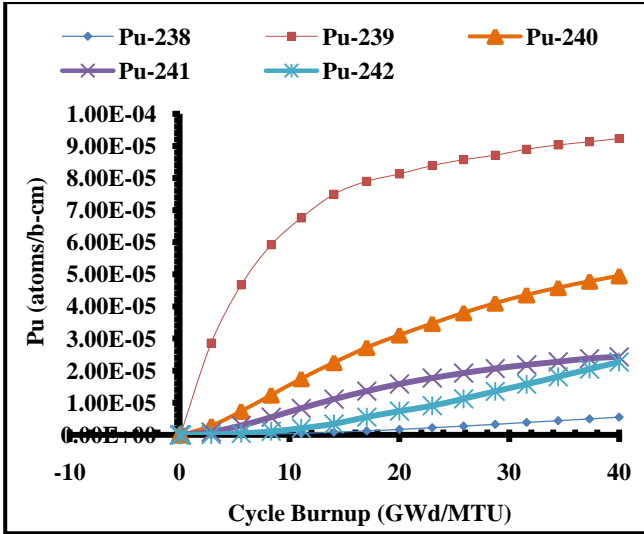


Figure 14. Plutonium isotopes concentration (atoms/barn-cm) with burnup (GWd/MTU) over full core

Figure 15 illustrates  $^{235}\text{U}$  (atom/b-cm) for three different assemblies with enrichment 2.05, 3.55, and 4.15% without burnable poisons or Gadolinia rods, the results show the level of  $^{235}\text{U}$  up to 40 (GWd/MTU).

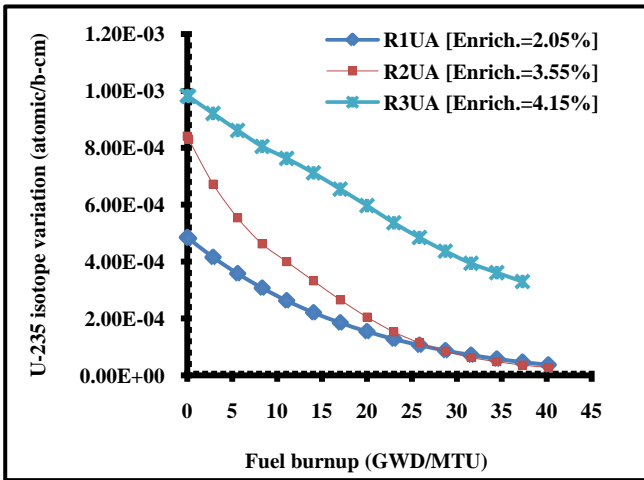


Figure 15.  $^{235}\text{U}$  concentrations (atoms/barn-cm) with burnup (GWd/MTU) of three regions contain pure  $\text{UO}_2$  only in the full core

Figure 16: illustrates  $^{235}\text{U}$  for two assemblies with initial enrichment 3.55% with and without burnable poison, the results indicate that  $^{235}\text{U}$  in assembly with 20 burnable rods per assembly have higher values, which indicate the effect of burnable poison in reducing fuel burnup and increasing the cycle length.

Figure 17 illustrates  $^{235}\text{U}$  concentrations (atoms/barn-cm) with burnup (GWd/MTU) of two assemblies containing Gadolinia rods with different enrichment (10% and 6%) in full core. At the beginning of the cycle assembly contains 10% Gadolinia rods have lower concentration than assembly contains 6% but at 12 GWd/T Gadolinia rods burns due to higher absorption cross section.

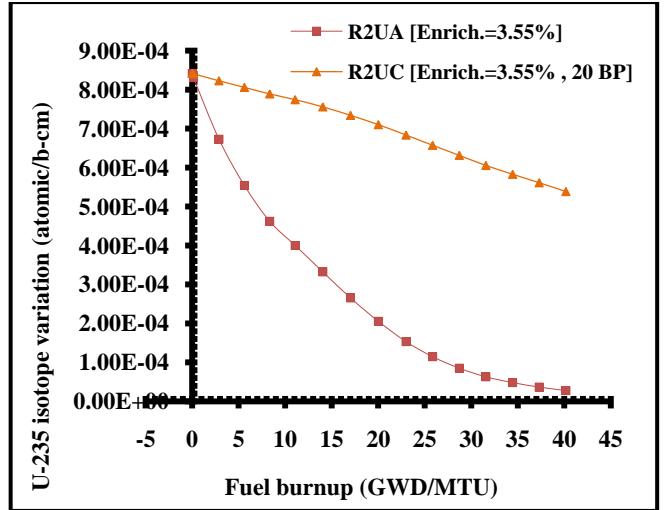


Figure 16.  $^{235}\text{U}$  concentrations (atoms/barn-cm) with burnup (GWd/MTU) of two regions with and without burnable absorber rods in full core

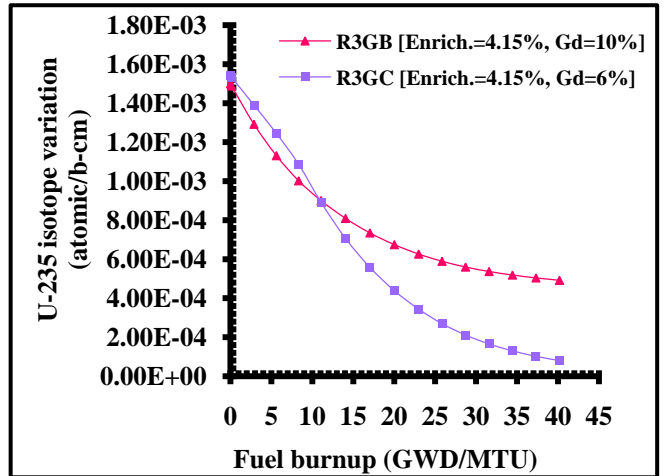


Figure 17.  $^{235}\text{U}$  concentrations (atoms/barn-cm) with burnup (GWd/MTU) of two regions contain Gadolinia rods with different enrichment (10% and 6%) in full core

Table 2. Delayed neutron fraction and prompt neutron life time for the reactor

Parameter	Present Result	Reference [1]
Delayed neutron fraction, $\beta_{\text{eff}}$ (%)	0.67	0.69
Prompt neutron lifetime, $\ell$ [Normal base load operation] ( $\mu\text{s}$ )	16.7	15.3

## 5. Conclusions

- MCNP6 computer code is used to design a computer model to the reactor core; the model includes reactor core, water cooling, neutron reflector, thermal shield and pressure vessel.
- Reactor effective multiplication factor and radial power distribution are in good agreement with the reactor design document.

- The results indicate that the reactor could achieve a fuel cycle of 24 months for the first initial core loading.
- Kinetic parameters such as delayed neutron fractions and prompt neutron life time are in good agreement with the reference.

---

## REFERENCES

- [1] Design Control Document for The US-APWR (Chapter 4 Reactor), MUAP- DC004 Revision 4 August 2013.
- [2] <http://www.world-nuclear.org/information-library/nuclear-fuel-cycle/nuclear-power-reactors/advanced-nuclear-power-reactors.aspx>.
- [3] Mitsubishi Fuel Design Criteria and Methodology, MUAP-07008-P-A Rev. 2, (Proprietary) and MUAP-07008-NP-A Rev.2 (Non-Proprietary), July 2013.
- [4] US-APWR Fuel System Design Evaluation, MUAP-07016-P Rev.4 (Proprietary) and MUAP-07016-NP Rev.4 (Non-Proprietary), August 2013.
- [5] US-APWR Fuel System Design Parameters List, MUAP-07018-P Rev.0 (Proprietary) and MUAP-07018-NP Rev.0 (Non-Proprietary), December 2007.
- [6] INTERNATIONAL ATOMIC ENERGY AGENCY, IAEA-TECDOC-844, "Characteristics and use of uranium-gadolinia fuels", 1995.
- [7] Pelowitz, D. B., MCNP6TM USER'S MANUAL Version 1.0, Manual Rev. 0, Los Alamos National Laboratory Report, LA-CP-13-00634, Rev. 0, May 2013.
- [8] T. Goorley, et al., "Initial MCNP6 Release Overview", Nuclear Technology, 180, p. 298-315, December 2012.
- [9] Chadwick M.B., et. al, "ENDF/B-VII.1: Nuclear Data for Science and Technology: "Cross Sections, Covariances, Fission Product Yields and Decay Data", Nuclear Data Sheets 112, 2011.
- [10] T. Goorley, "MCNP6.1.1-Beta Release Notes", LA-UR-14-24680, 2014.
- [11] MCNP5: X-5 Monte Carlo Team, "MCNP - Version 5, Vol. I: Overview and Theory", LA-UR-03-1987, 2003.
- [12] MCNPX: D.B. Pelowitz, Ed., "MCNPX User's Manual Version 2.7.0" LA-CP-11-00438, 2011.
- [13] U.S. Nuclear Regulatory Commission, Standard Review Plan for the Review of Safety Analysis Reports for Nuclear Power Plants, NUREG-0800, Section 4.2, March 2007.
- [14] General Design Criteria for Nuclear Power Plants, NRC Regulations Title 10, Code of Federal Regulations, 10 CFR Part 50, Appendix A.
- [15] American Society of Mechanical Engineers Boiler and Pressure Vessel Code Section III.
- [16] W. J. O'Donnell and B. F. Langer, Fatigue Design Basis for Zircaloy Components, Nuclear Science and Engineering 20, pp.1-12, 1964.
- [17] D. Hardie and M.W. Shanahan, Stress Reorientation of Hydrides in Zirconium 2.5% Niobium, Journal of Nuclear Materials 55, pp.1-13, 1975.
- [18] FINDS: Mitsubishi PWR Fuel Assemblies Seismic Analysis Code, MUAP-07034-P Rev.4 (Proprietary) and MUAP-07034-NP Rev.4 (Non-Proprietary), June 2013.
- [19] Evaluation Results of US-APWR Fuel System Structural Response to Seismic and LOCA Loads, MUAP-08007-P Rev.2 (Proprietary) and MUAP-08007-NP Rev.2 (Non-Proprietary), December 2010.
- [20] Mitsubishi Fuel Design Criteria and Methodology, MUAP-07008-P (Proprietary) and MUAP-07008-NP (Non-Proprietary), Rev. 2, July 2010.
- [21] Calculational and Dosimetry Methods for Determining Pressure Vessel Neutron Fluence, NRC Regulatory Guide 1.190, March 2001.
- [22] Oak Ridge National Laboratory, DOORS3.2: One, Two- and Three Dimensional Discrete Ordinates Neutron/Photon Transport Code System, RSICC Computer Code Collection CCC-650.
- [23] G. R. Keepin, et al., Delayed Neutrons from Fissionable Isotopes of Uranium, Plutonium and Thorium, Physical Review 107, 1044, 1957.
- [24] Liu, Y.S., et al., ANC - A Westinghouse Advanced Nodal Computer Code, WCAP-10965-P-A (Proprietary), and WCAP-10966-A (Non-Proprietary), September 1986.
- [25] X-5 Monte Carlo Team, MCNP - A General N-Particle Transport Code, Version 5 - Volume I: Overview and Theory, LA-UR-03-1987, Los Alamos National Laboratory, April 2003.
- [26] Validation of the MHI Criticality Safety Methodology, MUAP-07020, December 2007.
- [27] Guide for Validation of Nuclear Criticality Safety Calculational Methodology, NUREG/CR-6698, January 2001
- [28] International Handbook of Evaluated Criticality Safety Benchmark Experiments, NEA/NCS/DOC (95) 03/IV, September 2006 Edition.
- [29] Calculation Methodology for Reactor Vessel Neutron Flux and Fluence, MUAP-09018-P Rev.1 (Proprietary) and MUAP-09018-NP Rev.1 (Non-Proprietary), October 2009.
- [30] O'Grady, Eileen (2008-09-19). "Luminant seeks new reactor, 3rd Texas filing". Reuters. Retrieved 2008-09-19.
- [31] "Mitsubishi delays certification of APWR". World Nuclear News. 12 November 2013. Retrieved 15 November 2013.
- [32] "The US Advanced Pressurized Water Reactor". Mitsubishi Nuclear Energy Systems. Retrieved 15 November 2013.
- [33] "Japan to Cancel Plan to Build More Nuclear Plants". New York Times. May 10, 2011.
- [34] "EU-APWR passes EUR assessment". World Nuclear News.

22 October 2014. Retrieved 30 October 2015.

- [35] "Tsuruga 2 sits on active fault, NRA concludes". World Nuclear News. 26 March 2015. Retrieved 30 October 2015.

Copyright © 2021 The Author(s). Published by Scientific & Academic Publishing

This work is licensed under the Creative Commons Attribution International License (CC BY). <http://creativecommons.org/licenses/by/4.0/>